

# Hierarchy Influenced Differential Evolution: A Motor Operation Inspired Approach

Shubham Dokania<sup>1</sup>, Ayush Chopra<sup>1</sup>, Feroz Ahmad<sup>1</sup> and Anil Singh Parihar<sup>1</sup>

<sup>1</sup>Delhi Technological University, New Delhi, India

shubham.k.dokania@gmail.com, {ayushchopra\_2k14, ferozahmad\_2k14, anil}@dtu.ac.in

**Keywords:** Differential Evolution, Metaheuristics, Continuous Optimization, Hierarchical Influence

**Abstract:** Operational maturity of biological control systems have fuelled the inspiration for a large number of mathematical and logical models for control, automation and optimisation. The human brain represents the most sophisticated control architecture known to us and is a central motivation for several research attempts across various domains. In the present work, we introduce an algorithm for mathematical optimisation that derives its intuition from the hierarchical and distributed operations of the human motor system. The system comprises global leaders, local leaders and an effector population that adapt dynamically to attain global optimisation via a feedback mechanism coupled with the structural hierarchy. The hierarchical system operation is distributed into local control for movement and global controllers that facilitate gross motion and decision making. We present our algorithm as a variant of the classical Differential Evolution algorithm, introducing a hierarchical crossover operation. The discussed approach is tested exhaustively on standard test functions as well as the CEC 2017 benchmark. Our algorithm significantly outperforms various standard algorithms as well as their popular variants as discussed in the results.

## 1 Introduction

Evolutionary algorithms are classified as metaheuristic search algorithms, where possible solution elements span the  $n$ -dimensional search space to find the global optimum solution. Over the years, natural phenomena and biological processes have laid the foundation for several algorithms for control and optimization that have highlighted their applicability in solving intricate optimization problems. For instance, at the cellular level in the E.Coli Bacterium, there is sensing and locomotion involved in seeking nourishment and avoiding harmful chemicals. These behavioral characteristics fuelled the inspiration for the Bacterial Foraging Optimization algorithm (Passino, 2002)(Onwubolu and Babu, 2013). Particle Swarm Optimization (Kennedy and Eberhart, 1995) is a swarm intelligence algorithm based on behavior of birds and fishes that models these particles as they traverse an  $n$ -dimensional search space and share information in order to obtain global optimum. From a biological control point, the human brain represents one of the most advanced architectures and several research attempts seek to mimic its functional accuracy, precision and efficiency. The brain function activities can be broadly classified into 2 cate-

gories: sensory and motor operations. Sensory cortical functions inspired the concept of neural networks that are being scaled successfully in deep learning to solve vast amount of problems.

The human motor function represents a distributed neural and hierarchical control system. It can be clas-

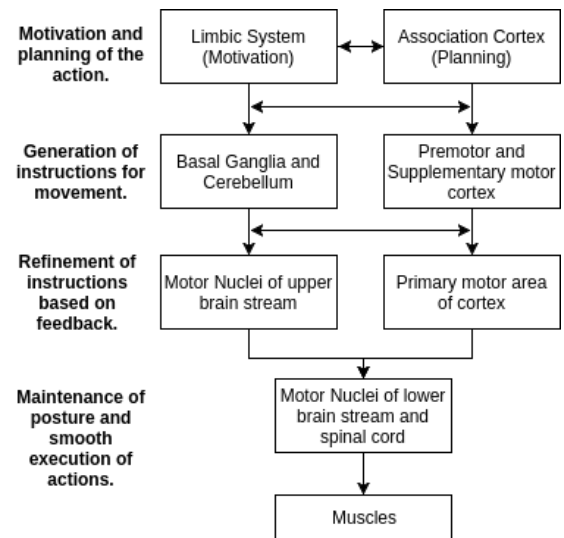


Figure 1: Hierarchy of Motor Control in Humans

sified as having local control functions for movement as well as higher level controllers for gross motion and decision making. The execution of motor operation involves distributed brain structures at different levels of hierarchy. These include the pre-frontal cortex, motor cortex, spinal cord, anterior horn cells etc (Shaw et al., 1982). For executing an action sequence, a sequence of actions is implemented by a string of subsequences of actions each implemented in a different part of the body. The operational structure has been depicted in Figure 1 (Passino, 2005). For optimality of actions, neurons act in unison. The neurons in the motor cortex act like global leaders and send inhibitory or facilitatory influence over anterior horn cells, the local leaders, located in the spinal cord (Shaw et al., 1982). These local leaders are connected to muscle fibers, the effectors, through a peripheral nerve and neuromuscular junction. Efficient execution of task requires feedback based facilitation and inhibition of the effectors over the anterior horn cells. These sequence of operations realise the optimal convergence of the system leading to smooth motor execution.

The present work introduces an algorithm modelled intuitively on the distributed and hierarchical operation of the brain motor function.

The Classical DE Algorithm (Storn and Price, 1995), proposed by Storn and Price has been hailed as one of the premier evolutionary algorithms, owing to its simple yet effective structure (Das and Suganthan, 2011). However, in recent times, it has been criticized for its slow convergence rate and inability to effectively optimize multimodal composite functions (Das and Suganthan, 2011). This work focusses on supplementing the algorithm's performance through the introduction of hierarchical influence in the pipeline. The architecture enables the algorithm to control the flow of agents through the cumulative effect of global and local leaders in the hierarchy. The proposed approach, Hierarchy Influenced Differential Evolution (HIDE), has been subjected to exhaustive analysis on the hybrid and composite objective functions of the CEC 2017 benchmark (Awad et al., 2016). Comparison with the classical DE algorithm and its other popular variants including JADE and PSODE (Zhang and Sanderson, 2009) highlights the particular viability of the schemed approach in solving complex optimization tasks. We show that even with fixed parameters, HIDE is able to outperform adaptive architectures such as JADE by a respectable margin, as discussed in the result sections.

## 2 Classical Differential Evolution

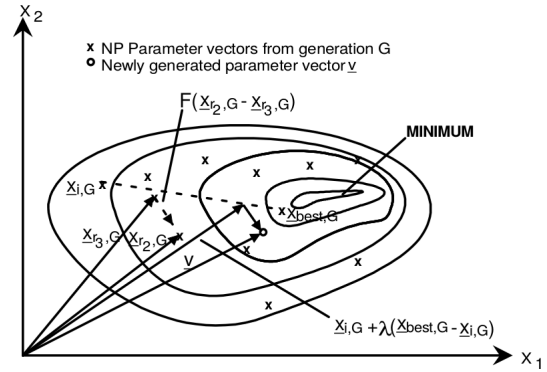


Figure 2: Motion planning of individuals in DE on two dimensional example of objective function.

The classical Differential Evolution (DE) algorithm is a population-based global optimization algorithm, utilizing a crossover and mutation approach to generate new individuals in the population for achieving optimum solutions (Das and Suganthan, 2011). For each individual  $x_i$  that belongs to the population for generation  $G$ , DE randomly samples three individuals from the population namely  $x_{r1,G}$ ,  $x_{r2,G}$  and  $x_{r3,G}$ . Employing these randomly chosen points, a new individual trial vector,  $v_i$ , is generated using equation (1):

$$v_i = x_{r1,G} + F(x_{r2,G} - x_{r3,G}) \quad (1)$$

Where,  $F$  is called the differential weight (Usually lies between  $[0, 1]$ ).

To obtain the updated position of the individual, a crossover operation is implemented between  $x_{i,G}$  and  $v_i$ , controlled by the parameter  $CR$  called the crossover probability. The value for  $CR$  always lies between  $[0, 1]$ .

## 3 Hierarchy Influenced Differential Evolution

Taking inspiration from the human motor system, we model the hierarchical motor operations in our optimization agents, where we define a global leader which influences the action of several distributed local leaders and the particle agents which act as the effectors. The global leader is analogous to the decision making and planning section in the motor system hierarchy whilst, the local leaders correspond to motion generators acting under the influence of the global leader.

The position of each particle in the population is affected by the influence of global leader and local leaders, while also being affected by a randomly chosen particle from the population to induce some stochasticity in the optimization pipeline. We first model the influence of the global leader on the local leaders and the influences of the local leaders on each population element using equation (3) and (4). We introduce a hierarchical crossover between the two influencing equations governed by a hierarchical crossover parameter  $HC$ .

Analogously to the brain motor operation as depicted in Figure 1, the update of particle positions requires generating feedback for the leaders as a part of the optimization procedure, and hence the local leaders and the global leader are updated based on their objective function value generated from the perturba-

tions in population particles. This series of events comprise of one optimization pass (one generation step). On execution of several optimization passes as described, the system is able to converge to an optimal configuration, analogous to the successful execution of the required task as shown in the final steps of Figure 1.

For each particle  $x_{i,G}$ ,  $i = 0, 1, 2, \dots, NP - 1$  for generation  $G$ , the trial vector  $x'_i$  of the particle, is governed by the hierarchical crossover operation and a mutation operation as follows :

$$u_i = \begin{cases} E_g, & \text{if } G < HC * G_t \\ E_l, & \text{otherwise} \end{cases} \quad (2)$$

$$E_g = g_L + F(x_{L_i,G} - x_{r,G}) \quad (3)$$

$$E_l = x_{L_i,G} + F(x_{i,G} - x_{r,G}) \quad (4)$$

for each dimension  $j$  of  $x_{j,i,G}$ :

$$x'_{j,i} = \begin{cases} x_{j,i,G} & \text{if } \text{rand}(0,1) < HC \\ u_{j,i} & \text{otherwise} \end{cases} \quad (5)$$

$$x_{i,G+1} = \begin{cases} x'_{i,G}, & \text{if } f(x'_{i,G}) < f(x_{i,G}) \\ x_{i,G}, & \text{otherwise} \end{cases} \quad (6)$$

where,

$G_t$  is the total number of generations,

$x_{i,G+1}$  is the vector position of  $x_{i,G}$  for next generation

$F$  is factor responsible for amplification of differential variation,

$f$  is the objective function,

$x_{i,G}$  is the current position of the individual for generation  $G$ ,

$u_i$  is the intermediate trial vector of the current individual,

$E_g$  represents the global and local leader interaction,

$E_l$  represents the local leader and effector interaction,

---

**Algorithm 1** Hierarchy Influenced Differential Evolution

---

```

1: procedure START
2:   Initialize parameters ( $HC, F, P, N_l, NP$ ).
3:   Generate initial global leader  $g_L$  as a random point.
4:   Generate  $N_l$  local leader points around  $g_L$  global leader.
5:   Generate  $NP$  points for population  $P$  around the local leaders using a Normal distribution with identity covariance.
6:   while Termination criteria is not met do
7:     for each individual  $x_{i,G}$  in  $P$  do
8:       Determine the corresponding local leader  $x_{L_i,G}$  from the set of all local leader based on nearest position.
9:       Let  $u = 0$  be an empty vector.
10:      Let  $G$  and  $G_t$  be the current generation and total generations of the procedure.
11:      if  $G < (HC * G_t)$  then
12:         $u_i = E_g$  from (3).
13:      else
14:         $u_i = E_l$  from (4).
15:      end if
16:       $x'_i = \text{BinomialCrossover}(u_i, x_{i,G}, CR)$ 
17:      if  $f(x'_i) < f(x_{i,G})$  then
18:        Replace  $x_{i,G}$  with  $x'_i$  in the next generation.
19:      end if
20:    end for
21:    Alter local leaders in each population cluster based on objective function value.
22:    Compute updated global leader  $g_L$ .
23:  end while
24: end procedure

```

---



---

**Algorithm 2** Binomial\_Crossover( $u, x, CR$ )

---

```

1: procedure START
2:   Let  $x' = 0$  be an empty vector.
3:   Select a random integer  $k = \text{irand}(\{1, 2, \dots, d\})$ ; where  $d$  = number of dimensions
4:   for each dimension  $j$  do
5:     if  $\text{random}(0, 1) < CR$  or  $j == k$  then
6:       Set  $x'_j = u_j$ 
7:     else
8:       Set  $x'_j = x_j$ 
9:     end if
10:  end for
11: end procedure

```

---

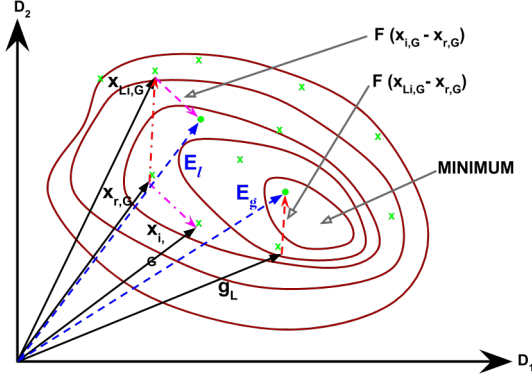


Figure 3: Hierarchical Decisive Motion planning of individuals in HIDE on two dimensional example of objective function. The position vectors resulting from the influence of global leader and local leaders are both represented as  $E_g$  and  $E_l$  on the contour of a two dimensional objective function.

$g_L$  is the global leader for generation  $G$ ,  
 $x_{L_i,G}$  is the position of the local leader for current individual,  
 $x_{r,G} \in P$ ;  $r \in [0,1, \dots, NP-1]$   
 $x'_{j,i}$  is the trial vector

$x_{r,G}$  is randomly chosen particle from the population to induce stochasticity. The hierarchical operation is affected by the global leader  $g_L$  and the local leader  $x_{L_i,G}$  through the parametric equations (3) and (4). Switching between the two is governed by the hierarchical crossover parameter  $HC$ .

### 3.1 Hierarchical Crossover

Convergence trend in HIDE is largely pivoted about (3) and (4), which in unison, lend a hierarchical structure to the algorithm. A successful optimization algorithm involves establishing a trade-off between exploration and exploitation. Achieving global optimization can be visualized as collaboration of two forces, exploration over a larger subspace followed by intensive exploitation over the resulting search space governed by clusters. Phase 1, involving (3) is marked by the interaction between the global and local leaders representing decision planning and facilitation of gross motion. This is followed by phase 2, involving (4) wherein the local leaders interact with and guide their effector population to control intricate motion over the constraint subspace to achieve smooth convergence. Robust convergence necessitates an optimal transition from phase 1 to phase 2 in the hierarchy.

This hierarchical transition is characterized by our proposed parameter,  $HC$ . The value of  $HC$  belongs to  $[0,1]$ . An optimal value for  $HC$  was observed experimentally to lie about one-quarter. For the purpose of our experiments, we have fixed  $HC$  to be 0.27. Thus, this defines a deterministic cut after 27% of the total generation budget. The crossover probability defined here was observed to be mostly 50% smaller in comparison to other DE variants.

The HIDE algorithm achieves a performance improvement in the early optimization phase ( $G < HC * G_t$ ) by replacing clusters of the initially generated candidate solutions with the locally best. This strategy rules out a number of mutation vectors that are more unfavorable in terms of performance gain. Additionally, by focusing on mutants of the globally best candidate solution the search space is explored rather quickly during this phase. After the population advances to  $HC * G_t$  generations, the algorithm changes its reference point (the trial vector) to the locally best candidate solutions of a certain cluster. That is, having approached a closer distance from the optimal, the algorithm is able to exploit the search space. Our proposition is complemented by the observations in our results section wherein we significantly outperform several popular algorithms on involved multi-modal hybrid and composite functions in higher dimensions.

## 4 Results and Discussions

All evaluations were performed using Python 2.7.12 with Scipy(Oliphant, 2007) and Numpy(Van Der Walt et al., 2011) for numerical computations and Matplotlib (Hunter, 2007) package for graphical rep-

Table 1: Algorithm Parameter Settings used for comparison

Algorithm	Parameter	Value
DE	$F$	0.5
	$CR$	0.9
PSODE	$w$	0.7298
	$\phi_p$	1.49618
	$\phi_g$	1.49618
	$F$	$r \in [0.9, 1.0)$
	$CR$	$r \in [0.95, 1.0)$
JADE	$p$	0.05
	$c$	0.1
HIDE	$HC$	0.27
	$F$	0.48
	$CR$	0.9
	$N_l$	5

Table 2: Objective Function Value for Dimension: 30

$f_{id}$	DE		JADE		PSO-DE		HIDE	
	best	mean	best	mean	best	mean	best	mean
$f_1$	100.001508	4334.43848	100.001338	100.056201	364.295574	4236.36321	<b>100.0</b>	<b>100.0</b>
$f_2$	40412441.0	5.1296e+19	<b>200.0</b>	1535352368	332899.0	9.59068e+11	<b>200.0</b>	<b>159855.5</b>
$f_3$	17926.8728	22131.5427	69304.9261	74080.7004	15792.5475	21683.2090	<b>3679.81159</b>	<b>8999.94726</b>
$f_4$	481.255055	519.422652	403.633939	<b>442.206911</b>	468.341175	479.341966	<b>400.004163</b>	443.016156
$f_5$	689.041352	737.79326	<b>667.50756</b>	<b>735.204027</b>	715.904429	746.548906	685.40454	738.842184
$f_6$	<b>643.626307</b>	652.582714	651.39169	655.142819	642.724237	655.106996	644.701241	<b>652.002395</b>
$f_7$	883.347367	962.591129	<b>779.907693</b>	<b>818.344111</b>	790.014281	854.285524	812.923573	856.90477
$f_8$	923.37426	967.251501	931.500175	<b>957.362003</b>	<b>915.414882</b>	960.486239	930.288539	964.11663
$f_9$	5652.48396	7878.78144	4953.05469	5146.60095	6018.41719	9042.41018	<b>4003.11807</b>	<b>4734.98436</b>
$f_{10}$	<b>3596.63104</b>	4536.98976	4012.72329	<b>4204.18969</b>	3934.60671	4863.74111	3793.78177	4346.74134
$f_{11}$	1162.40596	1184.63401	1152.74853	1174.58813	1165.14499	1189.17178	<b>1149.74849</b>	<b>1171.13041</b>
$f_{12}$	56679.4351	317650.613	24821.1717	58930.0902	10221.0774	161046.055	<b>9208.28924</b>	<b>41947.2226</b>
$f_{13}$	3002.02949	18794.8359	4276.90774	13775.8162	3871.27983	10612.2635	<b>1664.06241</b>	<b>2453.60697</b>
$f_{14}$	1773.18079	5502.16038	1496.21986	42868.9158	1555.45276	4029.80853	<b>1462.92685</b>	<b>1504.19151</b>
$f_{15}$	1860.43566	2484.68996	1688.05046	2222.67432	1651.74747	2223.06054	<b>1611.07440</b>	<b>1852.66177</b>
$f_{16}$	2517.43962	2827.00496	2344.19818	2621.61868	<b>2239.24272</b>	<b>2664.11466</b>	2298.04196	2691.67481
$f_{17}$	2321.17594	2604.52977	2062.89802	2546.99559	2107.43677	2457.34021	<b>1820.80664</b>	<b>2418.72383</b>
$f_{18}$	38987.2824	94156.3285	<b>11841.6081</b>	184888.162	62294.8532	118430.289	12578.0037	<b>23024.1119</b>
$f_{19}$	2043.46988	3010.23537	1959.71819	2156.95787	3049.52231	6840.40839	<b>1949.27171</b>	<b>1987.86676</b>
$f_{20}$	2625.53915	2864.83261	<b>2706.31444</b>	<b>2805.60006</b>	2619.99649	2895.10724	2753.80621	2966.03579
$f_{21}$	2412.08175	2504.77777	2414.52134	2456.71898	2431.74029	2478.84135	<b>2200.0</b>	<b>2442.73431</b>
$f_{22}$	2300.48179	5655.56932	<b>2300.0</b>	<b>4157.69878</b>	2307.72135	6811.06916	2300.00998	6795.24842
$f_{23}$	3050.65450	3572.96506	<b>2772.00202</b>	<b>2946.74932</b>	2764.92246	3199.87436	2883.27689	3543.83934
$f_{24}$	3104.62369	3290.69875	2891.55764	2965.22556	<b>2911.63347</b>	2983.77293	<b>2500.0</b>	2940.75997
$f_{25}$	2916.18065	2946.71175	2875.10684	2881.09138	2875.49884	2889.94367	<b>2874.17111</b>	<b>2877.48490</b>
$f_{26}$	4043.69140	6756.3724	2900.0	<b>3266.51098</b>	<b>2800.00780</b>	3273.12876	2900.0	3298.49053
$f_{27}$	3200.00585	3998.87649	3145.81035	<b>3189.82261</b>	3145.42523	3639.63413	<b>3132.81628</b>	3284.28897
$f_{28}$	3290.74402	3326.26398	<b>3100.0</b>	3131.02731	3195.48683	3225.59405	<b>3100.0</b>	<b>3115.50582</b>
$f_{29}$	3720.31459	4115.18580	<b>3305.31013</b>	<b>3626.88755</b>	3535.95229	3867.59306	3352.84505	3709.10237
$f_{30}$	3359.03076	3900.82666	<b>3263.49653</b>	3749.61072	3312.63502	3524.71447	3298.70464	<b>3421.71532</b>
w/t/l	2/0/28	0/0/30	8/2/20	11/0/19	4/0/26	1/0/29	15/2/13	17/0/13

Table 3: Objective Function Value for Dimension: 50

$f_{id}$	DE		JADE		PSO-DE		HIDE	
	best	mean	best	mean	best	mean	best	mean
$f_1$	5884574.87	367294248.5	136.072384	3708.75086	5811.21899	154233.646	<b>106.072862</b>	<b>3665.41927</b>
$f_2$	4.7181e+24	3.3649e+44	<b>2635725.0</b>	<b>5.0237e+26</b>	2.2121e+19	2.5445e+23	2.2799e+17	1.0072e+31
$f_3$	45520.9663	62237.2968	143481.793	156166.762	52308.4274	64435.2406	<b>44613.2999</b>	<b>58182.8373</b>
$f_4$	574.400328	801.384952	418.580378	470.113207	477.080964	574.528479	<b>400.005049</b>	<b>447.775413</b>
$f_5$	816.394775	843.258843	809.89948	834.13126	<b>778.59312</b>	831.066954	791.405194	<b>830.218472</b>
$f_6$	652.54191	655.794152	<b>633.21788</b>	<b>654.893828</b>	653.291336	658.183613	645.25633	656.060597
$f_7$	1109.02123	1263.03848	<b>889.036574</b>	<b>944.90319</b>	915.153525	1047.43879	989.957862	1186.2487
$f_8$	1139.27892	1175.8931	1118.3391	<b>1144.60474</b>	<b>1092.62639</b>	1159.03235	1100.4760	1168.5299
$f_9$	22196.3878	29218.7759	11958.2800	<b>13174.6623</b>	24753.0405	32233.9545	<b>10251.4763</b>	14752.7168
$f_{10}$	6228.49289	7289.18367	6054.70769	6833.30631	6207.79530	7055.59523	<b>6050.43437</b>	<b>6609.80456</b>
$f_{11}$	1170.85860	1258.51763	1202.69485	1232.20426	1206.15456	1252.93954	<b>1156.4396</b>	<b>1205.2544</b>
$f_{12}$	677263.079	16987989.9	<b>74784.6159</b>	530814.648	584300.698	3448448.79	126908.215	<b>494471.075</b>
$f_{13}$	6005.53530	16893.94992	2041.48812	4332.5945	1572.25297	<b>4301.82960</b>	<b>1484.76179</b>	7760.05613
$f_{14}$	38490.5323	174367.450	<b>2466.04705</b>	238838.470	16327.4231	67939.0002	2967.8184	<b>26290.3161</b>
$f_{15}$	2278.14122	26989.2555	13553.0418	25636.7696	3443.58734	<b>9167.26709</b>	<b>1938.20040</b>	14976.7218
$f_{16}$	2722.02601	3176.91690	<b>2345.40070</b>	<b>2916.56101</b>	2521.93881	3146.04527	2436.44933	2978.37746
$f_{17}$	2799.94977	3289.61565	2568.38357	2907.86927	2887.28110	3236.95792	<b>2561.37030</b>	<b>2874.96503</b>
$f_{18}$	264037.125	872072.477	36176.5867	<b>113941.317</b>	<b>26965.2851</b>	114846.121	260540.781	536454.326
$f_{19}$	10051.9124	20380.2571	2089.17225	7763.17234	9905.85082	16555.7569	<b>2013.12690</b>	<b>3609.25896</b>
$f_{20}$	2950.92319	3274.33401	3041.81309	3113.28946	2991.58929	3361.82394	<b>2495.03177</b>	<b>3080.13747</b>
$f_{21}$	2596.7256	2689.68836	2526.19089	2597.6771	2555.8788	2642.38159	<b>2447.75827</b>	<b>2570.91101</b>
$f_{22}$	9713.99324	10803.6537	10759.5967	11032.8809	8918.43626	10465.0224	<b>8181.4460</b>	<b>9755.0703</b>
$f_{23}$	3451.10494	4200.17442	2971.16064	3237.77866	2977.55496	3490.63975	<b>2851.65025</b>	<b>3162.31362</b>
$f_{24}$	3434.46502	3682.84670	3103.95517	3185.38267	<b>3036.79960</b>	<b>3158.33050</b>	3136.92774	3284.65609
$f_{25}$	3141.14488	3292.30344	2931.16295	2962.47175	2931.92695	3008.89535	<b>2931.14231</b>	<b>2954.76783</b>
$f_{26}$	4906.13284	7989.49096	<b>2900.0</b>	3346.87403	2900.44189	3653.75774	<b>2900.0</b>	<b>3262.66849</b>
$f_{27}$	3200.01070	3792.64558	3143.03805	3184.64635	3158.17823	3397.13032	<b>3141.01087</b>	<b>3176.01152</b>
$f_{28}$	3300.01082	3431.57091	<b>3240.72586</b>	<b>3288.25303</b>	3263.20714	3300.25760	3243.63199	3294.37323
$f_{29}$	3812.47551	4605.34953	<b>3533.94574</b>	<b>3956.83524</b>	3955.32453	4364.18129	3653.67555	3966.47195
$f_{30}$	3673.71196	5813.17375	3916.72571	4869.08933	3730.30935	5143.07870	<b>3346.48367</b>	<b>4747.88675</b>
w/t/l	0/0/30	0/0/30	8/1/21	9/0/21	4/0/26	3/0/27	17/1/12	18/0/12

resentation of the result data. This section is divided into two sub-sections: Section A provides description about the problem set used for analysis of algorithmic efficiency and accuracy, and section B comprises

of tabular and graphical data to reinforce the claim of superiority of the proposed approach.

Table 4: Objective Function Value for Dimension: 100

$f_{id}$	DE		JADE		PSO-DE		HIDE	
	best	mean	best	mean	best	mean	best	mean
$f_1$	3427212e+3	1380728e+4	141.263356	13516.69893	6067123.52	29751976.5	<b>122.398748</b>	<b>11708.8236</b>
$f_2$	4.196e+84	1.547e+112	8.737e+74	2.543e+87	<b>6.153e+66</b>	<b>3.211e+73</b>	3.8835e+80	8.891e+114
$f_3$	228808.969	262699.687	312244.360	332179.290	241427.723	257462.977	<b>220765.083</b>	<b>251901.109</b>
$f_4$	1975.65115	2752.24606	539.386275	677.05465	777.314462	836.965399	<b>531.169819</b>	<b>621.219143</b>
$f_5$	1223.53650	1286.15333	1249.19503	1307.11012	1248.41013	1310.88765	<b>1068.11742</b>	<b>1272.47682</b>
$f_6$	651.65013	657.84974	654.70934	659.421427	656.87704	662.31841	<b>642.33355</b>	<b>654.13275</b>
$f_7$	1614.00386	1920.79772	1367.06653	1536.35787	<b>1311.84975</b>	<b>1534.20776</b>	1562.37977	2076.70250
$f_8$	1595.41873	1736.36737	1672.56784	1768.08243	1678.12726	1761.9405	<b>1293.55211</b>	<b>1592.16298</b>
$f_9$	59726.5146	71986.0439	28906.9090	30336.7453	63640.3313	74961.2209	<b>23466.5750</b>	<b>27067.0295</b>
$f_{10}$	12005.8897	14725.3483	14227.8019	15355.6218	12937.0278	14972.9507	<b>11153.5868</b>	<b>13298.0921</b>
$f_{11}$	7540.6179	11481.2601	40447.5486	57228.6836	<b>3521.90152</b>	<b>4544.80401</b>	5380.43205	9916.34769
$f_{12}$	529993877	1881773e+3	3893556.27	<b>6415173.60</b>	26105108.9	41876679.1	<b>3680108.18</b>	10059039.6
$f_{13}$	7943.9249	508209.562	4622.69855	<b>8892.77599</b>	8246.51529	12675.8455	<b>2976.84135</b>	11376.9863
$f_{14}$	728122.833	1329183.17	<b>132194.795</b>	<b>365560.881</b>	548410.338	941547.524	234045.940	867160.306
$f_{15}$	2660.46578	181957.060	<b>1799.50650</b>	3362.50960	1899.07344	<b>2914.44348</b>	1976.78912	4485.4152
$f_{16}$	4749.25466	5847.82673	4817.48373	5632.3022	3852.7000	5228.6635	<b>3519.49494</b>	<b>4796.80272</b>
$f_{17}$	4397.49635	4958.41818	3842.20601	<b>4450.17742</b>	3790.72056	4730.99458	<b>3582.78588</b>	5463.21694
$f_{18}$	1357845.39	1938893.27	<b>146426.273</b>	<b>763318.822</b>	1004224.20	2315010.2	631040.146	1335739.59
$f_{19}$	2482.1701	26455.7069	2098.9496	4767.52953	2263.72515	3927.45994	<b>2071.07706</b>	<b>3664.15987</b>
$f_{20}$	4968.49743	5436.60405	5231.02648	5690.74899	5109.46056	5781.30083	<b>3627.77789</b>	<b>5228.43066</b>
$f_{21}$	3180.74665	3355.4783	2921.90012	<b>3085.6922</b>	<b>2885.57408</b>	3127.35683	2926.35039	3199.98618
$f_{22}$	17808.8977	19562.9866	19213.3756	20278.9290	18695.5223	20167.41374	<b>17548.3390</b>	<b>19547.1512</b>
$f_{23}$	4907.51964	5819.20786	<b>3352.5569</b>	4222.43689	3582.04355	4779.92124	3418.98320	<b>3609.0985</b>
$f_{24}$	5173.24940	5946.12042	4060.95130	4095.42951	<b>3801.36858</b>	<b>4042.42685</b>	3998.05402	4216.82489
$f_{25}$	4089.11891	4548.28576	<b>3153.48541</b>	<b>3236.61784</b>	3348.38226	3407.52658	3176.3038	3264.31853
$f_{26}$	8557.49856	20159.1145	2900.07737	11924.79947	3021.13602	8682.03543	<b>2900.00038</b>	<b>7867.5518</b>
$f_{27}$	3200.02335	3772.40915	<b>3194.80921</b>	3201.67073	3200.02417	3494.61813	3200.02354	<b>3200.02395</b>
$f_{28}$	4947.74515	5948.21315	<b>3295.12291</b>	<b>3340.28038</b>	3456.82843	3542.57130	3300.80769	3354.71733
$f_{29}$	6004.77442	7090.64254	5208.71172	5970.62868	5462.32863	6178.55906	<b>4541.19547</b>	<b>5739.29154</b>
$f_{30}$	7798.10621	202435555	<b>3584.97477</b>	10674.2173	3920.32703	<b>7139.46072</b>	3850.31709	15318.5546
w/t/l	0/0/30	0/0/30	8/0/22	8/0/22	5/0/25	6/0/24	17/0/13	16/0/14

#### 4.1 Problem Set Description

The set of objective functions considered for testing the proposed algorithm and compare its performance against classical DE and its variants PSODE and JADE have been taken from the CEC 2017 set of benchmark functions. Exhaustive comparisons and analysis have been depicted on dimensions  $D = 10, 30, 50$  and  $100$  for a clear understanding of the strengths of the proposed algorithm. Objective functions  $f_1 - f_3$  are simple unimodal functions and  $f_4 - f_{10}$  are multimodal functions with a high number of local optima values. Functions  $f_{11} - f_{20}$  are all hybrid functions using a combination of functions from  $f_1 - f_{10}$ . The set of composite function range from  $f_{21} - f_{30}$  and merges the properties of the sub-functions better while incorporating the basic functions as well as hybrid functions to increase complexity while maintaining continuity around the global optima.

#### 4.2 Parameter Settings

The work seeks to allow transparency in results by establishing a base for fair and clear comparisons in the analysis of the algorithms. The fixed values for the parameters have been depicted in table 1. The value of  $F$  and  $CR$  have been set as  $0.5$  and  $0.9$  for DE across all experiments, as recommended in the orig-

inal document in (Storn and Price, 1995), (Mezura-Montes et al., 2006), (Brest et al., 2006). The parameters for JADE were selected as suggested in the initial work (Zhang and Sanderson, 2009). The values of parameters for PSO-DE have been retained from (Liu et al., 2010) as it is one of the more cited and prestigious works. Also, we utilize the same parameter definitions for PSO as cited in this article by the initial authors in (Poli et al., 2007). The population size for initialised to  $100$  for all the algorithms as it is the uniformly recommended value by all of these papers. A total of  $100$  independent iterations were performed to obtain consistent result values to permit a uniform examination of the algorithm behaviour.

#### 4.3 Numerical and Graphical Results

In tables 2-4, the best and mean values obtained for the population agents in the simulation runs have been reported, and the optimum values for each objective function have been highlighted in **bold**. For the sake of clarity, the comparison results in each table have been summarized in "w/t/l" format wherein  $w$  represents the number of objective functions where the algorithm outperforms all other algorithms,  $t$  specifies the number of objective functions where it is tied as the best algorithm for the objective function and  $l$  represents the number of test functions where it does not finish first. The utilization of the evaluation met-

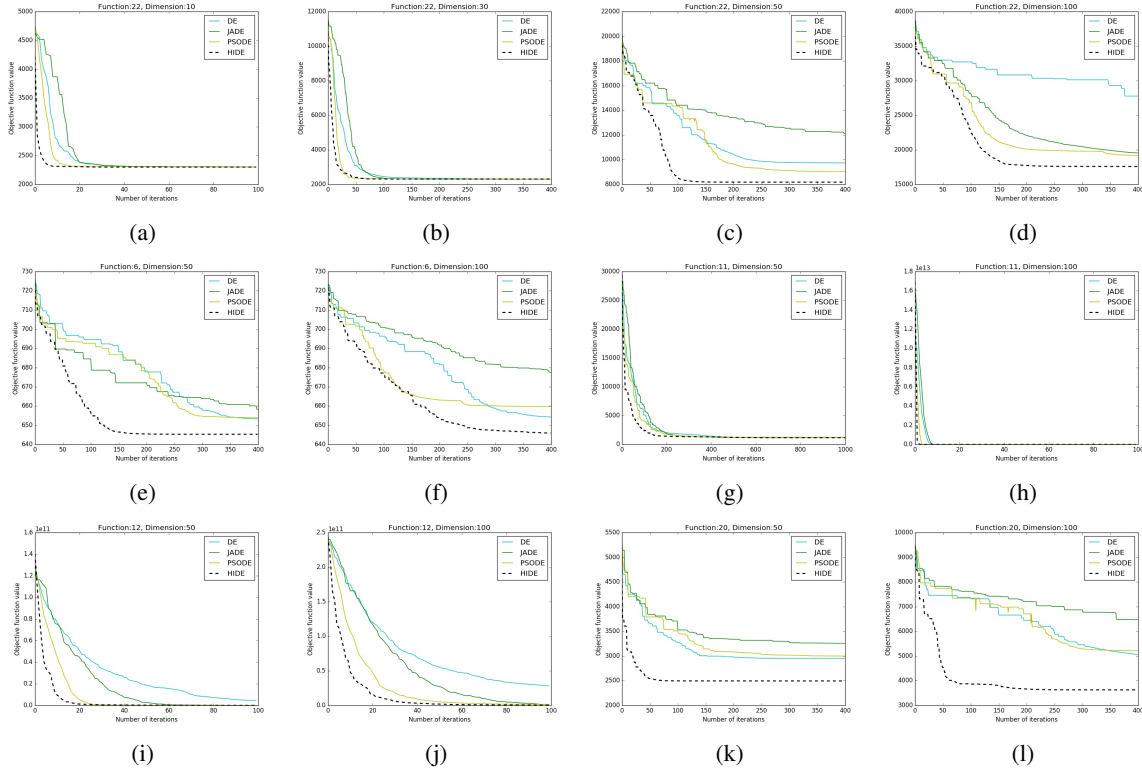


Figure 4: Comparative convergence profiles for test functions from CEC 2017 Benchmark over  $D = 10, 30, 50, 100$

ric facilitates a definitive comparison of the different algorithms under consideration.

As represented in Table 2, On  $D = 30$ , HIDE achieved maximum number of wins in both best and mean case (17 and 18 respectively). JADE achieved second position with 8 and 9 wins in the best and mean case. The decent performance of JADE can be attributed to the adaptive nature of its parameter selection which enables enhancement of its convergence rate.

The results for  $D = 50$  and  $D = 100$  (higher dimensions) have been summarized in tables 3 and 4. On  $D = 50$ , HIDE depicted exceptional performance, outperforming all other algorithms. It registered 17 wins in the best case and 18 wins in the mean case. Classical DE shows no wins in any case in high dimensional settings owing to its slow convergence rate and inability to attain global optimum thus highlighting the usefulness of the modifications introduced in the variants including HIDE. Similarly for  $D = 100$ , HIDE again outperforms all other algorithms by an appreciable margin. From a functional standpoint, It would be worthwhile to highlight that HIDE outperformed the other 3 compared algorithms on majority on the composite and hybrid functions, particularly on the higher dimensional settings. The efficiency of HIDE can be attributed to the hierarchical

nature of crossover selection and concurrency in vector configurations at the higher hierarchy levels. The tabular results reinforce the fact that HIDE outperforms JADE, PSODE and DE. On close analysis, it can be witnessed that HIDE falls behind the other algorithms on a small fraction of unimodal functions such as  $f_5, f_7$  on lower dimensions due to fast convergence during early stages of execution. However, the performance of higher dimensions, particularly on the more involved functions highlights utility for real world problems.

The tabular results are complemented through the graphical representations in Figure 4. For the sake of clarity, representations of higher dimensional problems span more number of iterations than those for lower dimensional settings. Analysis of the plots clearly depicts that HIDE shows better convergence rate as compared to other algorithms. As the analysis transcends to higher dimensional settings, the proposed approach outperforms the other algorithms on majority of the objective functions with respect to both convergence rate and optimality. the superiority of our algorithm in higher dimensions (50 and 100) is clearly evident from Figure 4 (c,d,g,h,k,l). Figure 4 (a,b,i,j) depict that for functions where HIDE and the other variants may depict similar trends on lower dimensions, HIDE eventually excels and surpasses

them in higher dimensions in most scenarios. Almost all figures are representative of a faster convergence rate for HIDE on higher dimensions. This remarkable trait in HIDE enhances its utility for high dimensional problems where fast convergence to global optimum value is required, hence making it superior to the other considered algorithms and several variants of the DE algorithm.

## 5 Conclusion

Differential Evolution has been regarded as one of the most successful optimization algorithms and over the years, several variants have been proposed to enhance its convergence rate and performance. In the present work, we introduced a hierarchy influenced variant of the classical DE algorithm and modeled the same on the brain motor operation. The algorithm was characterized by global leader, local leaders and an effector population. The global leader and distributed local leaders interacted to facilitate gross motion via a greedy exploration strategy. The local leaders and their effectors interacted to control intricate motion for smooth convergence. A hierarchical crossover parameter was introduced to characterize the hierarchical transition between the two interactions. The influence of the vector configurations at the higher levels of hierarchy enabled the algorithm to avoid local minima in most objective functions. The same is complemented through our result observations wherein we significantly outperform several popular algorithm on complex multimodal functions in higher dimensional settings. Our proposed approach has sought to establish a viable tradeoff between fast optimization, robust convergence and low number of control parameters. The performance analysis of the algorithm highlights the particular effectiveness of the proposed approach on high dimensional hybrid and composite functions. The observed results provide sufficient motivation to extend the scope of the work to complex high dimensional real life problems including image enhancement, traveling salesman problem and flexible job-shop scheduling.

## REFERENCES

- Awad, N., Ali, M., Liang, J., Qu, B., and Suganthan, P. (2016). Problem definitions and evaluation criteria for the cec 2017 special session and competition on single objective real-parameter numerical optimization. *Technical Report*.
- Brest, J., Greiner, S., Boskovic, B., Mernik, M., and Zumer, V. (2006). Self-adapting control parameters in differential evolution: A comparative study on numerical benchmark problems. *IEEE transactions on evolutionary computation*, 10(6):646–657.
- Das, S. and Suganthan, P. N. (2011). Differential evolution: A survey of the state-of-the-art. *Evolutionary Computation*, *IEEE Transactions on*, 15(99):4–31.
- Dorigo, M. and Stützle, T. (2010). Ant colony optimization: overview and recent advances. In *Handbook of metaheuristics*, pages 227–263. Springer.
- Hunter, J. D. (2007). Matplotlib: A 2d graphics environment. *Computing In Science & Engineering*, 9(3):90–95.
- Kennedy, J. and Eberhart, R. (1995). Particle swarm optimization. In *Neural Networks, 1995. Proceedings., IEEE International Conference on*, volume 4, pages 1942–1948 vol.4.
- Liu, H., Cai, Z., and Wang, Y. (2010). Hybridizing particle swarm optimization with differential evolution for constrained numerical and engineering optimization. *Appl. Soft Comput.*, 10(2):629–640.
- Mezura-Montes, E. n., Velázquez-Reyes, J., and Coello Coello, C. A. (2006). A comparative study of differential evolution variants for global optimization. In *Proceedings of the 8th Annual Conference on Genetic and Evolutionary Computation, GECCO '06*, pages 485–492, New York, NY, USA. ACM.
- Oliphant, T. E. (2007). Python for scientific computing. *Computing in Science & Engineering*, 9(3):10–20.
- Onwubolu, G. C. and Babu, B. (2013). *New optimization techniques in engineering*, volume 141. Springer.
- Passino, K. M. (2002). Biomimicry of bacterial foraging for distributed optimization and control. *IEEE control systems*, 22(3):52–67.
- Passino, K. M. (2005). *Biomimicry for optimization, control, and automation*. Springer Science & Business Media.
- Poli, R., Kennedy, J., and Blackwell, T. (2007). Particle swarm optimization – an overview.
- Shaw, D. M., Kellam, A., and Mottram, R. (1982). Brain sciences in psychiatry. In Shaw, D. M., Kellam, A., and Mottram, R., editors, *Brain Sciences in Psychiatry*. Butterworth-Heinemann.
- Storn, R. and Price, K. (1995). *Differential evolution-a simple and efficient adaptive scheme for global optimization over continuous spaces*, volume 3. ICSI Berkeley.
- Van Der Walt, S., Colbert, S. C., and Varoquaux, G. (2011). The numpy array: a structure for efficient numerical computation. *Computing in Science & Engineering*, 13(2):22–30.
- Zhang, J. and Sanderson, A. C. (2009). Jade: adaptive differential evolution with optional external archive. *IEEE Transactions on evolutionary computation*, 13(5):945–958.